JOURNAL OF GUIDANCE, CONTROL, AND DYNAMICS
Vol. 23, No. 2, March–April 2000

Vibration Suppression of Flexible Beams with Bonded Piezotransducers Using Wave-Absorbing Controllers

A. Yousefi-Koma* and G. Vukovich†
Canadian Space Agency, St. Hubert, Quebec J3Y 8Y9, Canada

A new wave-absorbing controller is designed for active control of smart structures. First, a novel dynamic wave model of piezosensors (as strain and strain rate sensors) is introduced. Second, a new wave state-space model of an integrated smart structure, consisting of a flexible beam with bonded piezosensors and piezoactuators for different collocated and noncollocated configurations, is derived. After defining output and input wave functions, a control system is then designed based on pushing the ratio of aggregate output to aggregate input wave functions toward zero. A simple proportional integral (PI) realization of the controller is introduced that depends only on the mechanical parameters of system and can be easily designed and employed. Whereas the controller is very easy to design and implement, results show its effectiveness.

I. Introduction

THERE have been numerous investigations on the modeling of flexible structures, particularly flexible beams, which are common elements of large structures and robotics. Because of the complexity of the equations of motion, discretization techniques are frequently used to construct a finite-dimensional system of ordinary differential equations. However, reducing the infinite-dimensional distributed systems to a finite-dimensional system (discretization) causes some problems, such as spillover[1] and sensitivity to small parameter perturbation of the structure.[2] Another limitation of discretization methods is that a great many modes may need to be considered, especially if it is desired to control the vibrations of large flexible structures or over a wide frequency range.[3]

An alternative to discretization techniques is distributed modeling, such as wave modeling of flexural motion. Wave modeling is suitable for many flexible structures, such as beams, plates, etc., that can serve as waveguides, thus allowing the response of the flexible system to be viewed as propagating flexural waves.[4]

Dynamic wave modeling of flexible structures can be used to design controllers based on wave absorption. Application of wave-absorbing controllers (WAC) in flexible structures has been studied in the recent years. To date WAC has been used primarily in active control systems with point sensors and actuators such as strain gauges and torque motors.[5–7] For example, Tanaka and Kikushima[8] designed a wave controller for flexible beams using an electrodynamic exciter and gap sensors. Fujii and Ohtsuka[9] also applied this method to a flexible beam with a torque motor actuator and strain gauge sensors. Because traveling waves are, in nature, distributed continuous phenomena, it is appropriate to employ distributed sensors and actuators in wave-based control systems. Among a number of possible choices, one of the suitable transducers is the distributed piezoelement. There is little literature on the application of WAC for smart structures using piezoelements. Pines and von Flotow[10] developed a wave controller for smart structures using piezoceramic actuators to control high-frequency acoustic waves of a flexible beam; however the sensors were point sensors, that is, strain gauges. On the other hand, in most previous literature,[7] the final expressions of wave controllers were highly nonlinear with half-differentiator and integrator elements that made it very difficult to realize actual implementation in the time domain. In addition, the wave method was most often used for high-frequency, for example, acoustics and noise control.

Received 17 December 1997; revision received 1 October 1998; accepted for publication 3 August 1999.

*Research Scientist, Directorate of Spacecraft Engineering; aghil.yousefi-koma@space.gc.ca.

†Director, Directorate of Spacecraft Engineering.

Based on the idea and the methodology introduced by von Flotow and Schäfer[6] and Pines and von Flotow,[10] in this research an easy design active control system was found for control of smart structures with bonded distributed piezoelectric sensors and actuators that can also be implemented for low-frequency vibration control. New dynamic wave models of distributed piezotransducers are developed, whereas, as mentioned earlier, in the previous literature most often point transducers were used.[5] Deriving the wave equations of the piezosensors as both strain and strain rate sensors eliminates the need for differentiation in the control system, which usually faces noise problems. Different collocated and noncollocated configurations of distributed piezoelectric sensors and actuators are studied, and a wave state-space model of the integrated smart structure is introduced. Finally, a proportional integral (PI) parameter-based approximation of the original nonlinear wave controller is introduced that is easy to design and implement with an effective active damping. The control gains can be obtained from a simple formula without knowledge of the dynamic model. This is a big advantage over most conventional controllers.

II. Dynamic Wave Modeling

A novel dynamic model of a smart structure is developed with respect to traveling waves. The smart structure consists of a flexible beam with distributed piezoelectric sensors and actuators.

A. Flexural Vibrations

The flexural vibration of an Euler–Bernoulli beam in the Laplace domain can be expressed by the following[9]:

$$\frac{\partial^4}{\partial x^4} v(x, s) + \frac{\rho_b s^2}{E_b I_b} v(x, s) = 0 \tag{1}$$

where v is the vertical displacement of the beam; E_b, I_b, and ρ_b are elastic modulus, moment of inertia of the cross section, and mass per length of the flexible beam, respectively; and s is the Laplace variable. The solution of Eq. (1) describes the transverse vibration of the flexible beam that can be expressed in the frequency domain using the Fourier transform

$$v(x, \omega) = A_1 e^{-i\mu x} + A_2 e^{-\mu x} + B_1 e^{i\mu x} + B_2 e^{\mu x} \tag{2}$$

where

$$\mu = \sqrt{\omega/\alpha}, \qquad \alpha = \sqrt{E_b I_b/\rho_b} \tag{3}$$

A_1, A_2, B_1, and B_2 are constants that can be obtained from the boundary conditions, and $v(x, \omega)$ can also be written in terms of so-called flexural waves, as defined by Pines and von Flotow[10]:

$$v(x, \omega) = a_1(x, \omega) + a_2(x, \omega) + b_1(x, \omega) + b_2(x, \omega) \tag{4}$$

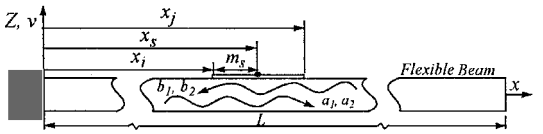

Fig. 1 Piezosensor on the flexible beam.

where

$$a_1(x, \omega) = A_1 e^{-i\mu x}, \qquad a_2(x, \omega) = A_2 e^{-\mu x}$$
$$b_1(x, \omega) = B_1 e^{i\mu x}, \qquad b_2(x, \omega) = B_2 e^{\mu x} \tag{5}$$

where subscript 1 represents traveling waves and subscript 2 evanescent waves for which amplitudes decay exponentially with x. The directions of the wave elements are as shown in Fig. 1. Here a_1 and a_2 are waves traveling in the positive x direction, and b_1 and b_2 represent waves in the negative direction. A wave function can be defined by the summation of the wave elements [Eq. (4)].

We define a wave state vector $\boldsymbol{w}$ at position x_i as

$$\boldsymbol{w}_i \equiv [a_1(x_i, \omega) \quad a_2(x_i, \omega) \quad b_1(x_i, \omega) \quad b_2(x_i, \omega)]' \tag{6}$$

where the superscript prime denotes the transpose of a vector or matrix. A physical state vector $\boldsymbol{s}$ at position x_i can be defined as

$$\boldsymbol{s}_i \equiv [v(x_i, \omega) \quad \theta(x_i, \omega) \quad M(x_i, \omega) \quad V(x_i, \omega)]' \tag{7}$$

where θ, M, and V are slope, bending moment, and shear force of the flexible beam, respectively. These two vectors are related by a coefficient matrix $\boldsymbol{H}$ as follows:

$$\boldsymbol{s}_i = \boldsymbol{H}\boldsymbol{w}_i \tag{8}$$

where

$$\boldsymbol{H} = \begin{bmatrix} 1 & 1 & 1 & 1 \\ -i\mu & -\mu & i\mu & \mu \\ -E_b I_b \mu^2 & E_b I_b \mu^2 & -E_b I_b \mu^2 & E_b I_b \mu^2 \\ -i E_b I_b \mu^3 & E_b I_b \mu^3 & i E_b I_b \mu^3 & -E_b I_b \mu^3 \end{bmatrix} \tag{9}$$

As described by von Flotow and Schäfer[6] using the definition of the wave state vector [Eq. (6)] the dynamic state space equation of the wave can be written as

$$\frac{\mathrm{d}\boldsymbol{w}}{\mathrm{d}x} = \eta \boldsymbol{w}, \qquad \eta = \mu \begin{bmatrix} -i & 0 & 0 & 0 \\ 0 & -1 & 0 & 0 \\ 0 & 0 & i & 0 \\ 0 & 0 & 0 & 1 \end{bmatrix} \tag{10}$$

and the wave state vectors at positions x_i and x_j can be related as

$$\boldsymbol{w}_j = \boldsymbol{T}_{ij}\boldsymbol{w}_i \tag{11}$$

where the spatial transition matrix $\boldsymbol{T}_{ij}$ is given by

$$\boldsymbol{T}_{ij} = \begin{bmatrix} e^{-ik_{ij}} & 0 & 0 & 0 \\ 0 & e^{-k_{ij}} & 0 & 0 \\ 0 & 0 & e^{ik_{ij}} & 0 \\ 0 & 0 & 0 & e^{k_{ij}} \end{bmatrix} \tag{12}$$

and k_{ij} is a dimensionless parameter given by

$$k_{ij} = (x_j - x_i)\mu \tag{13}$$

B. Strain and Strain Rate Piezosensors

In this section a new dynamic wave model of distributed piezosensor is developed. Piezoelements can be used as strain and strain rate sensors. In this study polarized hemopolymer of vinylidene fluoride (PVDF) piezofilm sensors[11] are attached to the surface of the flexible beam (Fig. 1). The output voltage and current of the piezosensor is proportional to the strain and strain rate, that is, moment and moment rate, respectively,[12]

$$V_s = \frac{E_s d_{31s} W_s}{C_s} \int_{(x_s - m_s)}^{(x_s + m_s)} \varepsilon \, \mathrm{d}x$$
$$= -\mathrm{sgn}(z) \frac{t_b E_s d_{31s} W_s}{2 E_b I_b C_s} \int_{(x_s - m_s)}^{(x_s + m_s)} M \, \mathrm{d}x \tag{14}$$

$$I_s = (E_s d_{31s} W_s) \int_{(x_s - m_s)}^{(x_s + m_s)} \frac{\mathrm{d}\varepsilon}{\mathrm{d}t} \mathrm{d}x$$
$$= -\mathrm{sgn}(z) \frac{t_b E_s d_{31s} W_s}{2 E_b I_b} \int_{(x_s - m_s)}^{(x_s + m_s)} \frac{\mathrm{d}M}{\mathrm{d}t} \mathrm{d}x \tag{15}$$

where E_s, W_s, d_{31s}, and C_s are elastic modulus, width, strain constant, and electric capacitance of the piezosensor, respectively; x_s and m_s are midpoint position and half-length of the piezosensor, respectively; ε and M are strain and bending moment, respectively; and t_b is beam thickness.

Using Eqs. (6–10) and expressing bending moment M with respect to the wave elements, we can express the output signals of the piezosensor by the wave state vectors as

$$V_s = -\mathrm{sgn}(z) \frac{t_b E_s d_{31s} W_s}{2 E_b I_b C_s} \left(M_0 \sqrt{\frac{\alpha}{\omega}} \right) [-i \quad -1 \quad i \quad 1] \{\boldsymbol{w}_j - \boldsymbol{w}_i\} \tag{16}$$

$$I_s = -\mathrm{sgn}(z) \frac{t_b E_s d_{31s} W_s}{2 E_b I_b} (M_0 \sqrt{\alpha\omega}) [1 \quad -i \quad -1 \quad i] \{\boldsymbol{w}_j - \boldsymbol{w}_i\} \tag{17}$$

where

$$M_0 \equiv E_b I_b \mu^2 \tag{18}$$

C. Moment Piezoactuators

The active effect of a pair of piezoactuators can be modeled as a pair of concentrated moments M_a (Fig. 2) at the end point of piezoactuators.[12,13] PZT piezoceramics (BM 532)[14] are bonded onto the surface of the beam and employed as the actuators. Introducing stiffness and thickness ratios as

$$\Upsilon \equiv \frac{(EWt)_b}{(EWt)_a} \qquad \tilde{t} \equiv \frac{t_a}{t_b} \tag{19}$$

where E, W, and t are elastic modulus, width, and thickness and subscripts b and a represent the flexible beam and the piezoactautor, respectively; we can write the induced moment M_a as[13]

$$M_a = (E_a W_a t_a t_b) \frac{\Upsilon(1 + \tilde{t})}{\Upsilon + 6(1 + 2\tilde{t} + \frac{4}{3}\tilde{t}^2)} \Lambda \tag{20}$$

where Λ is the strain induced by piezoelectric effect under the applied voltage V,

$$\Lambda = (d_{31a}/t_a) V \tag{21}$$

Using the methodology introduced by Pines and von Flotow[6] and considering the induced bending moment as the boundary conditions, we can use the following equations at the endpoints of the piezoactuators to incorporate M_a in the dynamic model:

$$\boldsymbol{s}_j^+ = \boldsymbol{s}_j^- + [0 \quad 0 \quad 1 \quad 0]' M_a \qquad \boldsymbol{s}_i^- = \boldsymbol{s}_i^+ + [0 \quad 0 \quad 1 \quad 0]' M_a \tag{22}$$

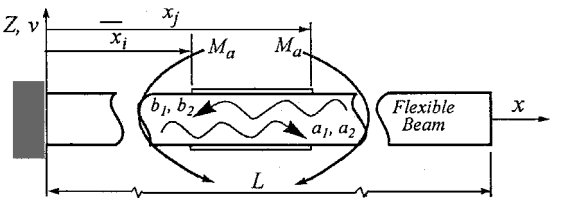

Fig. 2 Induced moments by piezoactuators.

where superscripts − and + denote left and right neighborhoods at the specific positions, respectively. Using Eqs. (8) and (11) we can write the preceding two equations as

$$\boldsymbol{H}\boldsymbol{w}_j^+ = \boldsymbol{H}\boldsymbol{T}_{ij}\boldsymbol{w}_i^+ + [0 \quad 0 \quad 1 \quad 0]' M_a \tag{23}$$

$$\boldsymbol{H}\boldsymbol{w}_i^- = \boldsymbol{H}\boldsymbol{w}_i^+ + [0 \quad 0 \quad 1 \quad 0]' M_a \tag{24}$$

Substituting $\boldsymbol{w}_i^+$ from Eq. (24) into Eq. (23) results in

$$[\boldsymbol{I} \quad -\boldsymbol{T}_{ij}] \begin{bmatrix} \boldsymbol{w}_j^+ \\ \boldsymbol{w}_i^- \end{bmatrix} = \Omega_{ij} M_a \tag{25}$$

where

$$\Omega_{ij} = (-\boldsymbol{T}_{ij} + \boldsymbol{I})\boldsymbol{H}^{-1}[0 \quad 0 \quad 1 \quad 0]' \tag{26}$$

D. Smart Structure

The dynamics of three different configurations of the smart structures with collocated and noncollocated transducers are studied in this section. The final dynamic equations are expressed via flexural waves of the sensing area.

1. Noncollocation Transducers

A smart structure with a pair of bonded piezoactuators (top and bottom) and two pairs of bonded piezosensors is considered (Fig. 3). The first pair of piezosensors (1 and 2) measures the strains, and the second pair (3 and 4) measures the strain rates. The total sensing area is the entire extent of x_1–x_6.

The wave state vectors at the end positions of the piezoactuators can be written [using Eq. (11)] as

$$\boldsymbol{w}_3^- = \boldsymbol{T}_{13}\boldsymbol{w}_1, \qquad \boldsymbol{w}_4^+ = \boldsymbol{T}_{46}^{-1}\boldsymbol{w}_6 \tag{27}$$

Substituting the Eq. (27) in Eq. (25) yields

$$\begin{bmatrix} \boldsymbol{I} & \boldsymbol{T}_{46}^{-1} & -\boldsymbol{T}_{34}\boldsymbol{T}_{13} \end{bmatrix} \begin{bmatrix} \boldsymbol{w}_6 \\ \boldsymbol{w}_1 \end{bmatrix} = \Omega_{34} M_a \tag{28}$$

We wish to express the dynamic equation of the smart structure with respect to the input and output wave vectors of the total sensing area ($\boldsymbol{w}_i$ and $\boldsymbol{w}_o$),

$$\boldsymbol{w}_i = [a_1(1) \quad a_2(1) \quad b_1(6) \quad b_2(6)]$$

$$\boldsymbol{w}_o \equiv [b_1(1) \quad b_2(1) \quad a_1(6) \quad a_2(6)]' \tag{29}$$

Thus, Eq. (28) can be rearranged as

$$\boldsymbol{S}_1\boldsymbol{w}_i + \boldsymbol{S}_2\boldsymbol{w}_o = \Omega_{34} M_a \tag{30}$$

where

$$\boldsymbol{S}_1 = \begin{bmatrix} -e^{-ik_{14}} & 0 & 0 & 0 \\ 0 & -e^{-k_{14}} & 0 & 0 \\ 0 & 0 & -e^{-ik_{46}} & 0 \\ 0 & 0 & 0 & -e^{-k_{46}} \end{bmatrix}$$

$$\boldsymbol{S}_2 = \begin{bmatrix} 0 & 0 & e^{ik_{46}} & 0 \\ 0 & 0 & 0 & e^{k_{46}} \\ -e^{ik_{14}} & 0 & 0 & 0 \\ 0 & -e^{k_{14}} & 0 & 0 \end{bmatrix} \tag{31}$$

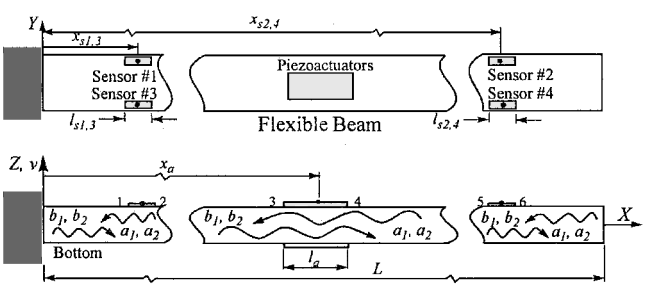

Fig. 3 Smart structure with noncollocated piezotransducers.

Expressing the output wave vector via the input wave vector [using Eq. (30)], we can write the final dynamic equation of the smart structure as follows:

$$\boldsymbol{w}_o = \boldsymbol{T}_{\text{ol}}\boldsymbol{w}_i + \Phi M_a \tag{32}$$

where

$$\Phi = \boldsymbol{S}_2^{-1}\Omega_{34} = \frac{1}{4M_0} \begin{bmatrix} e^{-ik_{14}} - e^{-ik_{13}} \\ e^{-k_{13}} - e^{-k_{14}} \\ e^{-ik_{36}} - e^{-ik_{46}} \\ e^{-k_{46}} - e^{-k_{36}} \end{bmatrix} \tag{33}$$

and $\boldsymbol{T}_{\text{ol}}$ is the open-loop transition matrix between output and input waves given by

$$\boldsymbol{T}_{\text{ol}} = -\boldsymbol{S}_2^{-1}\boldsymbol{S}_1 = \begin{bmatrix} 0 & 0 & e^{-ik_{16}} & 0 \\ 0 & 0 & 0 & e^{-k_{16}} \\ e^{-ik_{16}} & 0 & 0 & 0 \\ 0 & e^{-k_{16}} & 0 & 0 \end{bmatrix} \tag{34}$$

2. Collocation of Transducers of Unequal Length

In this case instead of four piezosensors we assume two long piezosensors are used (Fig. 4). Sensor 1 measures the strain and sensor 2 measures the strain rate. The numbering similar to the preceding case [Eq. (32)] without any change can be used for this case.

3. Collocation for Equal Length Transducers

This case is exactly like the preceding case except the length of the sensors and actuators are equal (Fig. 5). The two point pairs, 1 and 3 and 4 and 6, are geometrically superimposed, that is, $x_1 = x_3$ and $x_4 = x_6$; thus, Φ [Eq. (33)] can then be simplified to

$$\Phi = (1/4M_0)[(e^{-ik_{16}} - 1)(1 - e^{-k_{16}})(e^{-ik_{16}} - 1)(1 - e^{-k_{16}})]' \tag{35}$$

III. Frequency-Domain Wave Controller

In this section the wave-absorbing method is used to design an active control system for smart structures. As mentioned earlier, because only the local parameters of the system such as piezoelement lengths and their relative positions are considered, this controller is termed a local wave-absorbing controller (LWAC).

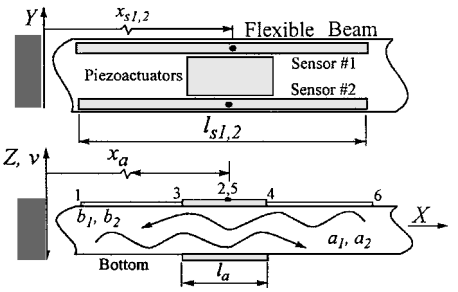

Fig. 4 Smart structure with unequal length collocated transducers.

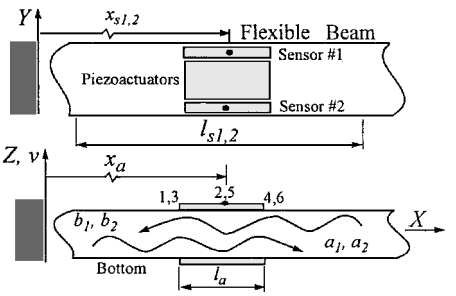

Fig. 5 Smart structure with equal length collocated transducers.

A. Noncollocated LWAC

A physical model of the smart structure with noncollocated transducers as shown in Fig. 3 is the subject of interest here. A feedback control loop in which the control voltage is proportional to the summation of the output currents of piezosensors 3 and 4 is used[15]:

$$V_a(\omega) = c(\omega)[I_{s3}(\omega) + I_{s4}(\omega)] \tag{36}$$

The other two sensors (1 and 2) are used for strain measurements. As mentioned earlier, the output voltage and current of a piezosensor are proportional to strain and strain rate respectively [Eqs. (14) and (15)]. Because $x_{s1} = x_{s3}$ and $l_{s1} = l_{s3}$ and $x_{s2} = x_{s4}$ and $l_{s2} = l_{s4}$ (where x_s and l_s are the length and the midpoint position of the piezosensors, see Fig. 3), the output voltages of piezosensors 1 and 2 are proportional to the time integration of output currents of piezosensors 3 and 4, respectively. This eliminates the need for integrating elements in the control loop.

Employing Eqs. (17), (20), and (36), we will then have the induced control moment

$$M_a(\omega) = c(\omega)\Psi\Gamma(\omega)\{(\boldsymbol{w}_2 - \boldsymbol{w}_1) + (\boldsymbol{w}_6 - \boldsymbol{w}_5)\} \tag{37}$$

where

$$\Psi = -\mathrm{sgn}(z)\frac{t_b^2(E_s d_{31s} W_s)(E_a d_{31a} W_a)}{2E_b I_b}\frac{\Upsilon(1+\tilde{t})}{\Upsilon + 6(1 + 2\tilde{t} + \frac{4}{3}\tilde{t}^2)} \tag{38}$$

where subscript a denotes the piezoactuator and $\boldsymbol{\Gamma}(\omega)$ is a vector as follows:

$$\boldsymbol{\Gamma}(\omega) \equiv [\boldsymbol{\Gamma}_1 \mid \boldsymbol{\Gamma}_2] \equiv (M_0\sqrt{\alpha\omega})[1 \quad -i \mid -1 \quad i] \tag{39}$$

where

$$\boldsymbol{\Gamma}_1 \equiv (M_0\sqrt{\alpha\omega})[1 \quad -i] \qquad \boldsymbol{\Gamma}_2 \equiv (M_0\sqrt{\alpha\omega})[-1 \quad i] \tag{40}$$

To obtain the closed-loop relation between the output and input waves, M_a [Eq. (37)] can be expressed in terms of $\boldsymbol{w}_i$ and $\boldsymbol{w}_o$ as follows:

$$M_a(\omega) = c(\omega)\Psi([-\boldsymbol{\Gamma}_1\delta_1 \mid \boldsymbol{\Gamma}_2]\boldsymbol{w}_i + [-\boldsymbol{\Gamma}_2\delta_2 \mid \boldsymbol{\Gamma}_1]\boldsymbol{w}_o) \tag{41}$$

where δ_1 and δ_2 are

$$\delta_1 \equiv \begin{bmatrix} 1 - e^{-ik_{12}} + e^{-ik_{15}} & 0 \\ 0 & 1 - e^{-k_{12}} + e^{-k_{15}} \end{bmatrix}$$

$$\delta_2 \equiv \begin{bmatrix} 1 - e^{ik_{12}} + e^{ik_{15}} & 0 \\ 0 & 1 - e^{k_{12}} + e^{k_{15}} \end{bmatrix} \tag{42}$$

The input and output waves, that is, $\boldsymbol{w}_i$ and $\boldsymbol{w}_o$, are given by Eq. (29). Substituting M_a from Eq. (41) into Eq. (30) gives the final expression of output wave vector with respect to the input wave vector:

$$\boldsymbol{w}_o = \left[(\boldsymbol{I} - c(\omega) \quad \Psi \quad \Phi \quad \mu_2)^{-1}(\boldsymbol{T}_{\mathrm{ol}} + c(\omega) \quad \Psi \quad \Phi \quad \mu_1)\right]\boldsymbol{w}_i \tag{43}$$

where

$$\mu_1 \equiv [-\boldsymbol{\Gamma}_1\delta_1 \mid \boldsymbol{\Gamma}_2], \qquad \mu_2 \equiv [-\boldsymbol{\Gamma}_2\delta_2 \mid \boldsymbol{\Gamma}_1] \tag{44}$$

Thus, the closed-loop transition matrix between the output and input wave vectors can be defined as

$$\boldsymbol{T}_{\mathrm{cl}} = \left[\boldsymbol{I} - c(\omega) \quad \Psi \quad \Phi \quad \mu_2\right]^{-1}\left[\boldsymbol{T}_{\mathrm{ol}} + c(\omega) \quad \Psi \quad \Phi \quad \mu_1\right] \tag{45}$$

Ignoring the evanescent elements of the wave function, that is, elements with subscript 2, that decay exponentially with x, the aggregate wave function input into the sensing area W_{Ti} and the aggregate output wave function from the sensing area W_{To} are defined as (Fig. 6):

$$W_{Ti} = a_1(1) + b_1(6), \qquad W_{To} = a_1(6) + b_1(1) \tag{46}$$

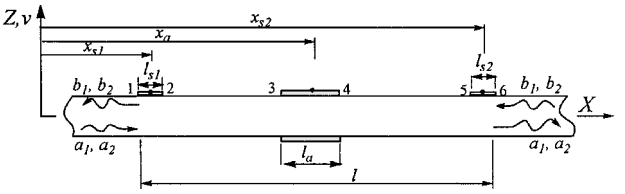

Fig. 6 Input and output traveling waves.

Thus, using Eqs. (43) and (45), we have

$$W_{To} = [\boldsymbol{T}_{\mathrm{cl}}(1,1) + \boldsymbol{T}_{\mathrm{cl}}(3,1)]a_1(1) + [\boldsymbol{T}_{\mathrm{cl}}(1,3) + \boldsymbol{T}_{\mathrm{cl}}(3,3)]b_1(6) \tag{47}$$

To simplify the complicated elements of the closed-loop transition matrix $\boldsymbol{T}_{\mathrm{cl}}$, the following geometric assumptions are used for the lengths and placements of the transducers:

$$l_{s1,3} = l_{s2,4}, \qquad x_a = (x_{s1,3} + x_{s2,4})/2 \tag{48}$$

These reasonable assumptions also introduce some symmetry into some of the $\boldsymbol{T}_{\mathrm{cl}}$ elements. The simplified elements of $\boldsymbol{T}_{\mathrm{cl}}$ can then be written as

$$\boldsymbol{T}_{\mathrm{cl}}(1,1) = \boldsymbol{T}_{\mathrm{cl}}(3,3) = (\sqrt{\alpha\omega}\Psi/4\Delta)c(\omega)[(e^{-ik_{13}} - e^{-ik_{14}}) \times (1 - e^{-ik_{12}} + e^{-ik_{15}} - e^{-ik_{16}})] \tag{49}$$

and

$$\boldsymbol{T}_{\mathrm{cl}}(1,3) = \boldsymbol{T}_{\mathrm{cl}}(3,1) = (1/\Delta)\Big\{-e^{-ik_{16}} + (\sqrt{\alpha\omega}/4)\Psi c(\omega) \times [(e^{-ik_{14}} - e^{-ik_{13}})(1 + e^{-ik_{16}}) + ie^{-ik_{16}}(2e^{-k_{14}} - 2e^{-k_{13}} + e^{-k_{23}} + e^{k_{23}} - e^{-k_{24}} - e^{k_{24}})]\Big\} \tag{50}$$

where Δ is the determinant of $[\boldsymbol{I} - c(\omega) \quad \Psi \quad \mu_2]$. By the use of the preceding symmetric properties, Eqs. (46) and (47) yield

$$W_{To} = [\boldsymbol{T}_{\mathrm{cl}}(1,1) + \boldsymbol{T}_{\mathrm{cl}}(1,3)]W_{Ti} \tag{51}$$

which gives the final relation between aggregate output and input wave functions.

As the control criterion we push the ratio of aggregate output and input wave functions toward zero, and consequently, this causes a damping in the output wave amplitudes. This ratio can be written as follows using Eq. (51):

$$W_{To}/W_{Ti} = \boldsymbol{T}_{\mathrm{cl}}(1,1) + \boldsymbol{T}_{\mathrm{cl}}(1,3) \tag{52}$$

Thus, the control objective will be

$$W_{To}/W_{Ti} = 0 \tag{53}$$

Replacing $\boldsymbol{T}_{\mathrm{cl}}(1,1)$ and $\boldsymbol{T}_{\mathrm{cl}}(1,3)$ from Eqs. (49) and (50) and solving the preceding equations result in the final expression of the LWAC in the frequency domain:

$$1/c(\omega) = (\sqrt{\alpha\omega}/4)\Psi[(e^{-ik_{14}} - e^{-ik_{13}})(2 + e^{-ik_{15}} - e^{-ik_{12}})e^{ik_{16}} + i(2e^{-k_{14}} - 2e^{-k_{13}} + e^{-k_{23}} + e^{k_{23}} - e^{-k_{24}} - e^{k_{24}})] \tag{54}$$

B. Collocated LWAC (Unequal Length Transducers)

We now examine the case of a model with transducers of unequal length, as shown in Fig. 4. To use the equations derived in the preceding section, we assume this as a special case of noncollocation but with piezosensors extended to reach each other, that is, $x_2 = x_5$. The two piezosensors are the same, the one used for strain rate measurement (piezosensor 2) and the other for the strain measurement (piezosensor 1). The voltage command in this case is

$$V_a(\omega) = c(\omega)I_{s2}(\omega) \tag{55}$$

and $\boldsymbol{w}_i$ and $\boldsymbol{w}_o$ will be the same as in the earlier case. The geometric simplification assumption is

$$x_a = x_{s1} = x_{s2} \tag{56}$$

The control criterion is that of the preceding section, that is, $\theta(c) = 0$, and results in the following LWAC for this case:

$$1/c(\omega) = (\sqrt{\alpha\omega}/2)\Psi[(e^{-ik_{14}} - e^{-ik_{13}})e^{ik_{16}} + i(e^{-k_{14}} - e^{-k_{13}})] \tag{57}$$

C. Collocated LWAC (Equal Length Transducers)

For the smart structure model with collocated transducers of equal length, located at the same position (Fig. 5)

$$l_a = l_{s1} = l_{s2} \qquad x_a = x_{s1} = x_{s2} \tag{58}$$

In this case the control criterion, that is, $\theta(c) = 0$, leads to the collocated LWAC:

$$1/c(\omega) = (\sqrt{\alpha\omega}/2)\Psi[(1 - e^{ik_{16}}) + i(e^{-k_{16}} - 1)] \tag{59}$$

IV. Simplified LWAC

In general the wave-absorbing method produces controllers that are difficult to realize in practice due to the necessity for half-integrations and half-differentiations,[6,9,16] among other things. To more easily implement the LWACs in the time domain, some approximations of the controllers are needed.[6,17] In the following sections new techniques to obtain simple versions of the LWAC are developed.

A. Analytical Parameter-Based LWAC (APB LWAC)

We show that in the case of collocated piezotransducers with equal lengths it is possible to derive a simple analytical approximation of the LWAC, that is, $c(\omega)$ given by Eq. (59), that can be easily implemented in the time domain. For low frequencies and for short piezoelements, k_{16} is much less than 1, so that we can ignore the higher power terms of k_{16} that appear in the exponential expansion. This is the case of interest in most flexural vibration control systems (k_{16} value is examined in the next section for the model studied in this paper). Ignoring the higher orders of k_{16}, that is, powers greater than two, the exponential expansion of the local wave-absorbing controller, defined by Eq. (59), can be simplified to the following:

$$c(\omega) = \frac{2}{\Psi\sqrt{\alpha}}\frac{1}{\sqrt{\omega}}\left[\frac{\beta_{16}^2\omega/2 + i(2\beta_{16}\sqrt{\omega} - \beta_{16}^2\omega/2)}{4\beta_{16}^2\omega}\right] \tag{60}$$

where

$$\beta_{16} = k_{16}/\sqrt{\omega} = (x_6 - x_1)/\sqrt{\alpha} \tag{61}$$

This is an expression for the second order of expansion of $c(\omega)$. On substituting α and from β_{16} from Eqs. (3) and (61), respectively, $c(\omega)$ can be rewritten as follows:

$$c(\omega) = \left[\left(-\frac{1}{\Psi}\frac{1}{l_a}\right)\frac{1}{(i\omega)}\right] + \left[\frac{1}{\Psi}\frac{0.25}{\sqrt{\sqrt{E_b I_b/\rho_b}}}\frac{1}{\sqrt{\omega}}(1 - i)\right] \tag{62}$$

where $l_a = x_6 - x_1$ is the piezoactuator length. The first component is an integration operator $[1/(i\omega)]$. To simplify the realization, we ignore the imaginary part of the second component [Eq. (62)]. This simplification is examined in Sec. V in which the Bode plots show only a little error. If we are interested in vibration control around the first vibrational mode, which is true in many active vibrational control tasks, the second component can be written as

$$\frac{1}{\Psi}\frac{0.25}{\sqrt{\sqrt{E_b I_b/\rho_b}}}\frac{1}{\sqrt{\omega_1}} \tag{63}$$

Finally, from Eqs. (62) and (63), the approximation of the LWAC becomes a simple PI controller, the gains of which can be easily obtained from

$$\text{proportional gain} \equiv \frac{0.25}{\Psi\sqrt{\omega_1\sqrt{E_b I_b/\rho_b}}} \qquad \text{integral gain} \equiv -\frac{1}{\Psi l_a} \tag{64}$$

Because Ψ depends on only the parameters of the composite smart structure, the control gains can simply be calculated from knowledge of system physical parameters. As mentioned earlier [Eq. (36)], the input signal to this controller is the output currents of the piezosensors, that is, strain rate. Thus using a PI controller actually strain and strain rate are used to provide the control command. This approximation provides an analytical parameter-based (APB) LWAC design that can be easily implemented in practice. The controller gains can be obtained from a simple formula [Eq. (64)], which, unlike the usual dynamic model-based controllers such as linear quadratic regulator, requires no simulation process to obtain the control gains. This is a substantial advantage over conventional controllers.

B. Curve Fit Model (CFM) of LWAC

Another approach for approximation of the LWAC is particularly suitable for the cases for which analytical approximations are very difficult to obtain, for example, noncollocated LWAC. From the Bode plots of the LWAC, it is possible to find a suitable PI realization around the low-frequency range by curve matching of the original magnitude and phase plots. This enables us to implement the LWAC in the time domain. In the next section comparisons between the original LWAC and curve fit model (CFM) LWAC are made, and their performances for sample structures are compared.

V. Frequency- and Time-Domain Results of LWAC

In this section we study the performance of LWAC in both the frequency and time domains. A physical model of a smart structure consisting of a 1-m-long flexible aluminum beam 52 mm in width and 0.8 mm in thickness, PVDF piezofilm sensors[11] 13 mm in width and 0.028 mm in thickness, and a pair of identical PZT piezoceramic actuators (BM 532)[14] 25.4 mm in width and 0.3 mm in thickness is considered. For this configuration of smart structure, $\Psi = -2.22762 \times 10^{-9}$ N/V^2 and $\alpha = 1.1904$ m^2/s. LWAC and its simplified versions are then applied to active vibration control of the flexible beam with an initial tip displacement of 4 mm.

A. Collocation (Equal Length Transducers)

Piezosensors with the same length as the actuator length are used for this case of collocation: $l_{s1,2} = l_a = 150$ mm and $x_s = 500$ mm. Around the first mode frequency ($\omega_1 = 4.3085$ rad/s), $k_{16} = 0.2854$. Consequently, the APB LWAC that provides a PI approximation of the LWAC, designed in Sec. IV.A [Eq. (64)], is $\text{PI} \equiv -(6.6667/s) + 0.1104$. Figure 7 shows the Bode plot of the controller. APB LWAC performance is very close to that of the original LWAC, particularly for the frequencies around the first mode. Figure 8 shows that the controller shifts the peaks to the left and increases the damping of the system around the second mode, with little attenuation of the first modal amplitude (1 dB). The controller does not suppress the flexural vibration of the beam effectively, due to the short sensing area, that is, $l_s = 150$ mm.

B. Collocation (Unequal Length Transducers)

In this case two long piezosensors are used to sense the traveling waves: $l_{s1,2} = 800$ mm and $x_{s1,2} = 500$ mm. The CFM LWAC is $\text{PI} \equiv -(9.0/s) + 1.0$. The magnitude and phase of the controller with respect to the frequency are shown in Fig. 9. It is seen that for low frequencies, the CFM LWAC is close to the original LWAC. The dynamic response of the control system is compared with the open-loop response in the frequency domain in Fig. 10. The closed-loop system performance with the original and approximated controller are very close to each other in the low-frequency range. The LWAC provides large damping to the dynamic system. The closed-loop response of the smart structure to the initial tip displacement of 4 mm is shown and compared with that of the open loop in Fig. 11. The controller damps the flexural vibration quickly.

C. Noncollocation

The following configuration of the piezosensors is considered for this case (Fig. 3): $l_{s1,3} = l_{s2,4} = 200$ mm, $x_{s1,3} = 200$ mm, and $x_{s2,4} = 800$ mm.

The approximate model for the LWAC obtained from curve fitting the Bode diagrams (CFM LWAC) is $\text{PI} \equiv -(7.0/s) + 0.35$. Figure 12 shows the Bode plot of the controller. It can be seen that in the low-frequency range the controller behaves like a PI controller, the approximate and the original controller behaviors match

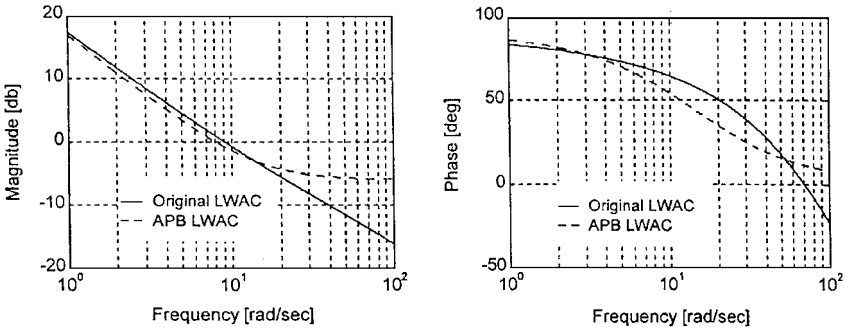

Fig. 7 Collocated LWAC: equal length transducers.

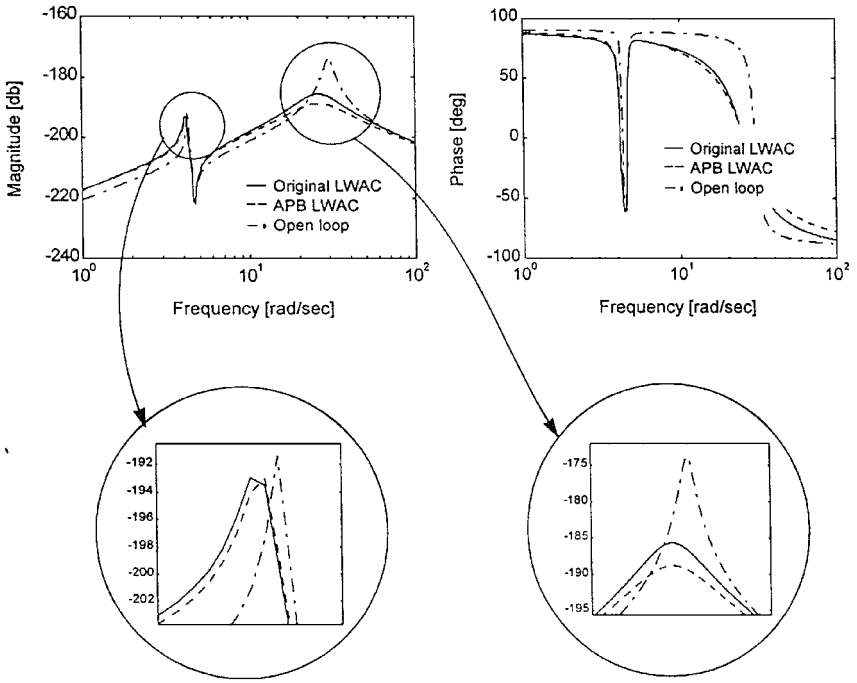

Fig. 8 Frequency response of the smart structure with the collocated LWAC: equal length transducers.

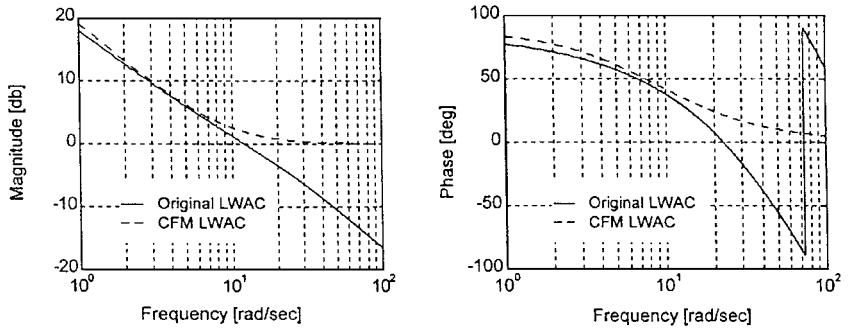

Fig. 9 Collocated LWAC: unequal length transducers.

quite well. The performance of the closed-loop control system is compared with the open loop in Fig. 13. The LWAC suppresses the vibration effectively, particularly in the low-frequency range. The first mode peak is decreased significantly in magnitude by 9 dB. The PI model of CFM LWAC performs very similarly to the original LWAC, and this simple approximation can be quite effective. The time-domain response of the flexible beam is shown in Fig. 14 with an initial tip displacement of 4 mm with and without control. Comparing the open-loop and closed-loop responses shows that the controller does indeed significantly damp the vibration.

D. Sensing Length Effect on the LWAC

The performance of the controlled smart structure with different lengths of the piezosensors studied in the preceding sections shows that the LWAC becomes much more effective in active vibration damping as the length of the sensing area increases. For example, in the case of covering 800 mm of the beam length, the controller provided the highest damping, whereas the lowest damping was for the collocation case with a piezosensor 150 mm in length. This effect and the effects of other parameters, such as structural length and stiffness, are studied by Yousefi-Koma and Vukovich.[18]

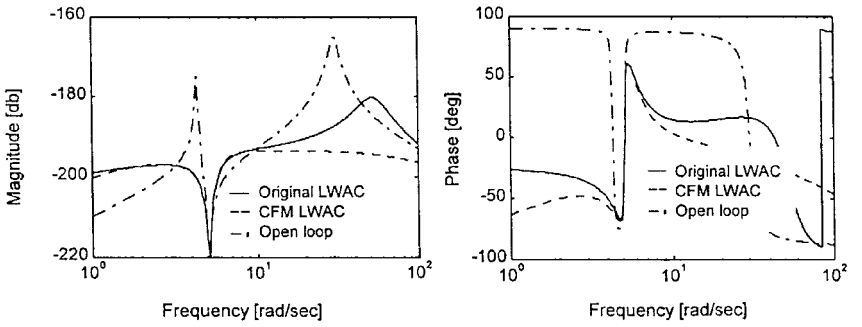

Fig. 10 Frequency response of the smart structure with the collocated LWAC: unequal length transducers.

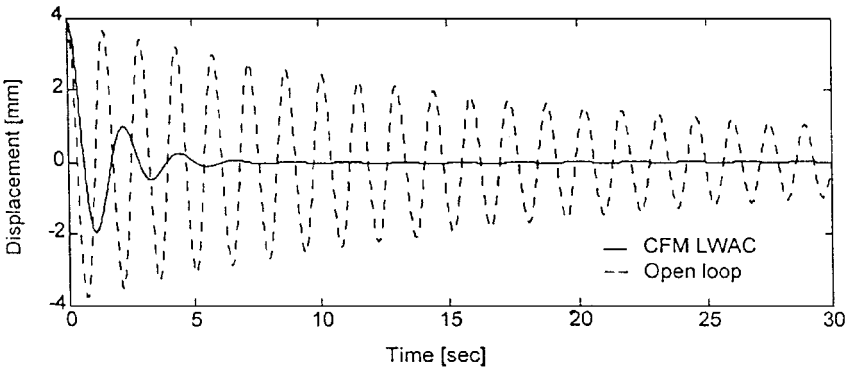

Fig. 11 Tip displacement of the smart structure with the collocated LWAC: unequal length transducers.

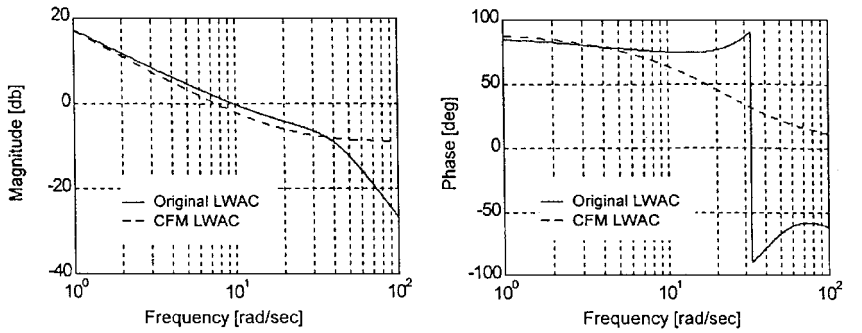

Fig. 12 Noncollocated LWAC.

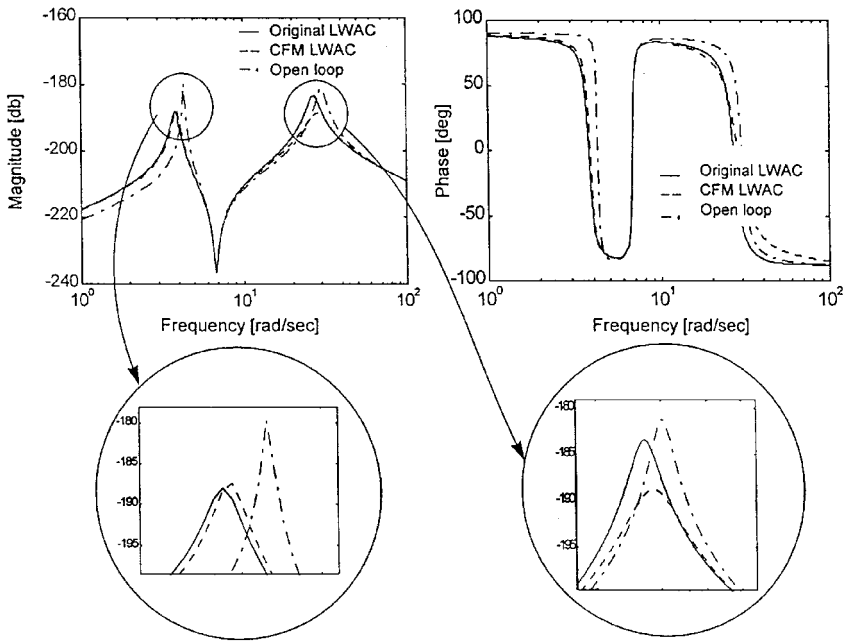

Fig. 13 Frequency response of the smart structure with the noncollocated LWAC.

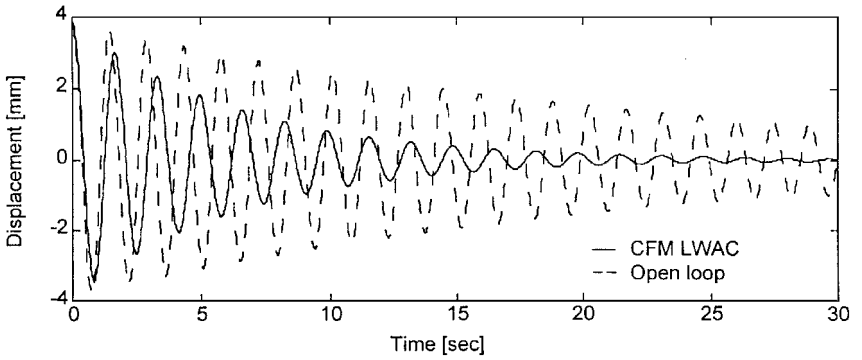

Fig. 14 Tip displacement of the smart structure with the noncollocated LWAC.

VI. Conclusions

A novel active wave control system for vibration suppression of smart structures was developed. Both sensors and actuators are of piezoelectric materials. After deriving a dynamic wave model of the distributed piezoelectric sensors for both strain and strain rate measurements, the need for differentiator terms in the control loop was eliminated, and, consequently, the controller is less sensitive to noises. By the use of aggregate output and aggregate input wave functions, a control criterion was introduced and employed to design the wave control system. Although the wave method is most often employed in active noise and acoustic control by previous researchers, the wave controller introduced here was capable of low-frequency vibration control as well. A new approximation of the nonlinear realization of the wave controller resulted in a parameter-based PI controller that can be easily implemented in practice. The frequency- and time-domain results showed that the controller could suppress the flexural vibrations effectively.

References

[1]Bass, R. W., and Zes, D., "Spillover, Nonlinearity, and Flexible Structures," *IEEE Proceedings of the 30th Conference on Decision and Control*, Inst. of Electrical and Electronics Engineers, New York, 1991, pp. 1633–1637.

[2]Miller, D. W., von Flotow, A., and Hall, S. R., "Active Modification of Wave Reflection and Transmission in Flexible Structures," *Proceedings of American Control Conference*, Inst. of Electrical and Electronics Engineers, New York, 1987, pp. 1318–1324.

[3]Mace, B. R., "Active Control of Flexural Vibrations," *Journal of Sound and Vibration*, Vol. 114, No. 2, 1987, pp. 253–270.

[4]Graff, K. F., "Wave Motion in Elastic Solids," *Clarendon Press*, Oxford Univ. Press, Ely House, London, 1975, pp. 140–155.

[5]von Flotow, A. H., "Traveling Wave Control for Large Spacecraft Structures," *Journal of Guidance, Control, and Dynamics*, Vol. 9, No. 4, 1986, pp. 462–468.

[6]von Flotow, A. H., and Schäfer, B., "Wave-Absorbing Controllers for a Flexible Beam," *Journal of Guidance, Control, and Dynamics*, Vol. 9, No. 6, 1986, pp. 673–680.

[7]Fujii, H., Ohtsuka, T., and Murayama, T., "Wave-Absorbing Control for Flexible Structures with Noncollocated Sensors and Actuators," *Journal of Guidance, Control, and Dynamics*, Vol. 15, No. 2, 1992, pp. 431–439.

[8]Tanaka, N., and Kikushima, Y., "Active Wave Control of a Flexible Beam (Fundamental Characteristics of an Active-Sink System and Its Verification)," *JSME International Journal*, Ser. 3, Vol. 35, No. 2, 1992, pp. 236–244.

[9]Fujii, H., and Ohtsuka, T., "Experiment of a Noncollocated Controller for Wave Cancellation," *Journal of Guidance, Control, and Dynamics*, Vol. 15, No. 3, 1992, pp. 741–745.

[10]Pines, D. J., and von Flotow, A. H., "Active Control of Bending Wave Propagation at Acoustic Frequencies," *Journal of Sound and Vibration*, Vol. 142, No. 3, 1990, pp. 391–412.

[11]Product Catalogue, Elf Atochem Sensors, Inc., Valley Forge, PA, 1992.

[12]Yousefi-Koma, A., "Active Vibration Control of Smart Structures Using Piezoelements," Ph.D. Thesis, Dept. of Mechanical and Aerospace Engineering, Carleton Univ., Ottawa, ON, Canada, Sept. 1997.

[13]Crawley, E. F., and de Luis, J., "Use of Piezoelectric Actuators as Elements of Intelligent Structures," *AIAA Journal*, Vol. 25, No. 10, 1987, pp. 1373–1385.

[14]Product Catalogue, Sensor Technology, Ltd., BM Hi-Tech Div., Collingwood, ON, Canada, 1996.

[15]Vukovich, G., and Yousefi-Koma, A., "A Non-Collocated Active Traveling Wave Control of Smart Structures Using Distributed Transducers," *5th IEEE International Conference on Control Applications*, Inst. of Electrical and Electronics Engineers, New York, 1996, pp. 297–302.

[16]Miller, D. W., and Hall, S. R., "Experimental Results Using Active Control of Traveling Wave Power Flow," *Journal of Guidance, Control, and Dynamics*, Vol. 14, No. 2, 1991, pp. 350–359.

[17]Yousefi-Koma, A., and Vukovich, G., "A Parameter Based Time Domain Design of Wave Absorbing Controller for Flexible Structures Using Piezoelectric Transducers," *Proceedings of SPIE's Symposium on Smart Structures and Materials*, International Society for Optical Engineering, Washington, 1996, pp. 600–607.

[18]Yousefi-Koma, A., and Vukovich, G., "Size and Stiffness Effects of Structures and Piezoelectric Transducers on Wave Controllers," *Proceedings of the 3rd IFAC Symposium on Intelligent Components and Instruments for Control Applications*, International Federation of Automatic Control, France, 1997, pp. 697–702.